Structural Engineering and Mechanics, Vol. 2, No. 2 (1994) 157-171
DOI: http://dx.doi.org/10.12989/sem.1994.2.2.157

Seismic behavior of fuel assembly for pressurized water reactor

Myung J. Jhung †

Power Reactor Mechanical Engineering, Korea Atomic Energy Research Institute
150 Dukjin-dong, Yusung-ku, Taejon 302-353, Korea

Won G. Hwang ‡

Department of Mechanical Engineering, Chonnam National University
Yongbong-dong 300, Puk-gu, Kwangju 500-757, Korea

Abstract. A general approach to the dynamic time-history analysis of the reactor core is presented in this paper as a part of the fuel assembly qualification program. Several detailed core models are set up to reflect the placement of the fuel assemblies within the core shroud. Peak horizontal responses are obtained for each model for the motions induced from earthquake. The dynamic responses such as fuel assembly deflected shapes and spacer grid impact loads are carefully investigated. Also, the sensitivity responses are obtained for the earthquake motions and the fuel assembly non-linear response characteristics are discussed.

Key words: reactor internals; reactor core; fuel assembly; pressurized water reactor; seismic behavior; operating basis earthquake; safe shutdown earthquake; spacer grid.

1. Introduction

The reactor core of a pressurized water reactor (PWR) is composed of several hundreds of assemblies of different kinds such as ordinary fuel assemblies and control element assemblies. They are rectangular beams supported by a fuel alignment plate and a core support plate at the top and bottom ends, respectively, immersed in coolant with very narrow spacings between adjacent assemblies. Thus, in an earthquake event, their vibratory motions as a whole cluster may have a complicated nature including non-linearity due to the effects of collisions between assemblies and dynamic interactions through fluid coupling forces.

Seismic safety qualification of the reactor core is one of the crucial issues in the seismic design of a PWR, and it should be secured that the structural integrity of the fuel assemblies and the control rod insertion capabilities be maintained against the design seismic loads. The procedure for core analysis is described briefly as follows. As the first step, reactor vessel motion is obtained from the reactor coolant system analysis in which a very simplified model of the internals and core is used. Subsequently, the reactor vessel motion is used as an input

† Senior Researcher
‡ Professor

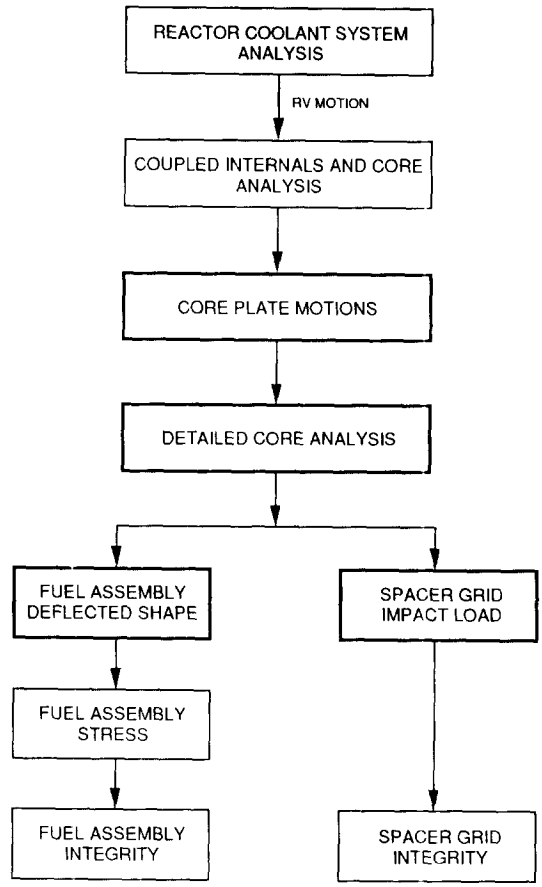

Fig. 1 Analysis procedure for fuel assembly seismic design.

to a coupled model of internals and core. In this model, only a lumped model of the core is used with a primary purpose to include interaction effects between the response of the fuel assemblies, core plates and core shroud. In the last step, core plates and core shroud motions from the coupled internals and core analysis are input to the detailed core model in which each fuel assembly is modeled individually. Fig. 1 illustrates the overall design analysis flow.

For the purpose of assessing seismic safety of the reactor core, the dynamic response of the fuel assemblies should be evaluated with a sufficient accuracy, which requires a well validated large scale analysis methodology or experiment. In this context, various experimental efforts have been made to understand dynamic characteristics of a reactor core (Chen 1975 and Queval, et al. 1991). But practically it is almost impossible to get the response by experiment because of difficulties of experimental setup or economical reasons. It necessitates the analytical study for the vibration characteristics of fuel assembly.

In the present study, a method for detailed seismic analysis of the reactor core is developed. The SHOCK computer code (Gabrielson 1966) which is used to solve the dynamic response of the lumped mass systems is updated to include the off-diagonal terms of the hydrodynamic masses in the equations of motion. Several detailed core models are set up to reflect the placement

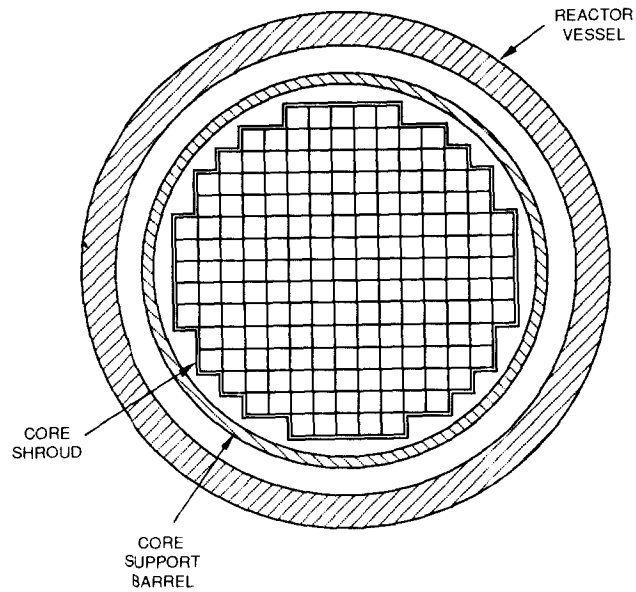

Fig. 2 Reactor core arrangement.

of the fuel assemblies within the core shroud. Peak horizontal responses are obtained for each model for the motions induced from earthquake. The dynamic responses such as fuel assembly deflected shapes and spacer grid impact loads are carefully investigated. Also, the sensitivity responses are obtained for the earthquake motions and the fuel assembly non-linear response characteristics are discussed.

2. Description of fuel assembly

The typical PWR core of 2825 MWt is composed of 177 fuel assemblies and 73 or more control element assemblies. The fuel assemblies are arranged to approximate a right circular cylinder with an equivalent diameter of 123 inches and an active length of 150 inches (Fig. 2). The fuel assembly, which provides for 236 fuel rod positions (16×16 array), includes 5 guide tubes welded to 11 spacer grids and is closed at the top and bottom by end fitting (Fig. 3). The guide tubes each displace four fuel rod positions and provide channels which guide the control element assemblies over their entire length of travel. In-core instrumentation is installed in the central guide tube of selected fuel assemblies. The in-core instrumentation is routed into the bottom of the fuel assemblies through the bottom head of the reactor vessel. The outer guide tubes, spacer grids and end fittings form the structural frame of the assembly.

The fuel spacer grids maintain the fuel rod array by providing positive lateral restraint to the fuel rod but only frictional restraint to axial fuel rod motion. The grids are fabricated from preformed Zircaloy or Inconel strips (the bottom spacer grid material is Inconel) interlocked in an egg crate fashion and welded together. Each cell of the spacer grid contains two leaf springs and four arches. The leaf springs press the rod against the arches to restrict relative motion between the grids and the fuel rods.

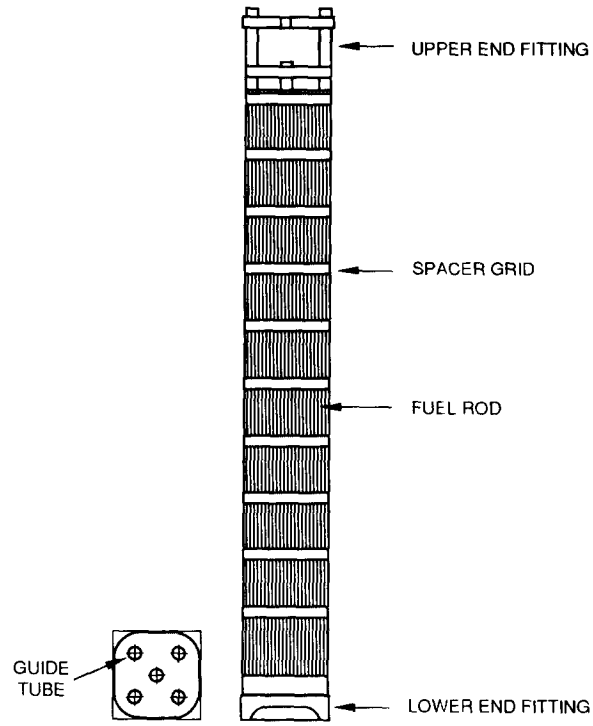

Fig. 3 Schematic diagram of fuel assembly.

3. Response to forced motions

Let us suppose that the displacements x on a structure are partitioned into two submatrices such that

$$x=\begin{bmatrix} x_a \\ x_b \end{bmatrix} \tag{1}$$

and the displacements x_b are forced to vary in a defined manner. Thus the displacements x_b are prescribed functions of time. This problem is practical importance in calculating the response of a structure to earthquake movement. The earthquake causes horizontal movement and rotation of the foundation, forcing the displacements on the structure to follow the earthquake movements. There are also many other practical applications where the structure is subjected to forced displacements rather than to applied forces. By using the partitioning in Eq. (1) the equations of motion can be accordingly partitioned into

$$\begin{bmatrix} m_{aa} & m_{ab} \\ m_{ba} & m_{bb} \end{bmatrix} \begin{bmatrix} \ddot{x}_a \\ \ddot{x}_b \end{bmatrix} + \begin{bmatrix} c_{aa} & c_{ab} \\ c_{ba} & c_{bb} \end{bmatrix} \begin{bmatrix} \dot{x}_a \\ \dot{x}_b \end{bmatrix} + \begin{bmatrix} k_{aa} & k_{ab} \\ k_{ba} & k_{bb} \end{bmatrix} \begin{bmatrix} x_a \\ x_b \end{bmatrix} = \begin{bmatrix} 0 \\ p_b \end{bmatrix} \tag{2}$$

where p_b represents the column matrix of unknown forces causing the displacements x_b. Taking the first in Eq. (2), we have

$$m_{aa}\ddot{x}_a+m_{ab}\ddot{x}_b+c_{aa}\dot{x}_a+c_{ab}\dot{x}_b+k_{aa}x_a+k_{ab}x_b=0$$

$$m_{aa}\ddot{x}_a+c_{aa}\dot{x}_a+k_{aa}x_a=-[m_{ab}\ddot{x}_b+c_{ab}\dot{x}_b+k_{ab}x_b]$$

or

$$m_{aa}\ddot{x}_a+c_{aa}\dot{x}_a+k_{aa}x_a=\bar{p}_a \tag{3}$$

where $\bar{p}_a=-[m_{ab}\ddot{x}_b+c_{ab}\dot{x}_b+k_{ab}x_b]$. The value $\bar{p}_a$ is known for the given displacements x_b and therefore the displacements x_a are calculated from Eq. (3). The forces p_b necessary to cause the required displacements x_b can be computed from the second of Eq. (2) and is

$$p_b=m_{ba}\ddot{x}_a+m_{bb}\ddot{x}_b+c_{ba}\dot{x}_a+c_{bb}\dot{x}_b+k_{ba}x_a+k_{bb}x_b \tag{4}$$

Alternately Eq. (2) can be written as

$$\begin{bmatrix} m_{aa} & m_{ab} \\ m_{ba} & m_{bb} \end{bmatrix}\begin{bmatrix} \ddot{x}_a \\ \ddot{x}_b \end{bmatrix}\equiv\begin{bmatrix} F_a \\ F_b \end{bmatrix} \tag{5}$$

where

$$\begin{bmatrix} F_a \\ F_b \end{bmatrix}=\begin{bmatrix} -(c_{aa}\dot{x}_a+c_{ab}\dot{x}_b+k_{aa}x_a+k_{ab}x_b) \\ -(c_{ba}\dot{x}_a+c_{bb}\dot{x}_b+k_{ba}x_a+k_{bb}x_b)+p_b \end{bmatrix} \tag{6}$$

and F_a and F_b are the spring and damping forces at nodes a and b, respectively. In a solution which is based on a direct integration of the equations of motion, the spring and damping forces are evaluated at each instant of time and then the accelerations are solved. Integration of the accelerations gives the velocities and displacements needed to reevaluate the accelerations for the next time step.

If the hydrodynamic couplings are considered in the analysis, the mass matrix is

$$m=m_s+m_h \tag{7}$$

where m_s and m_h are the structural and hydrodynamic mass matrices, respectively. Consider the two mass points with hydrodynamic couplings. Then Eq. (5) becomes

$$\begin{bmatrix} m_{aas}+m_{aah} & m_{ab} \\ m_{ba} & m_{bbs}+m_{bbh} \end{bmatrix}\begin{bmatrix} \ddot{x}_a \\ \ddot{x}_b \end{bmatrix}=\begin{bmatrix} F_a \\ F_b \end{bmatrix} \tag{8}$$

When there is no hydrodynamic coupling to any of the b nodes, then m_{ab} and m_{ba} become null and m_{bb} becomes m_{bbs}. Then Eq. (8) becomes

$$\begin{bmatrix} m_{aa} & 0 \\ 0 & m_{bbs} \end{bmatrix}\begin{bmatrix} \ddot{x}_a \\ \ddot{x}_b \end{bmatrix}=\begin{bmatrix} F_a \\ F_b \end{bmatrix}=\begin{bmatrix} -(c_{aa}\dot{x}_a+c_{ab}\dot{x}_b+k_{aa}x_a+k_{ab}x_b) \\ m_{bbs}\ddot{x}_b \end{bmatrix} \tag{9}$$

This Eq. (9) is used to correctly solve for $\ddot{x}_a$ and $\ddot{x}_b$. Let $F_b=m_{bbs}\ddot{x}_b$ where $\ddot{x}_b$ is the set of prescribed accelerations. Then $\ddot{x}_b=\ddot{x}_b$ if there is no hydrodynamic coupling to b nodes.

If, however, there is any hydrodynamic coupling to b nodes, then Eq. (8) is

$$\begin{bmatrix} m_{aa} & m_{ab} \\ m_{ba} & m_{bbs}+m_{bbh} \end{bmatrix}\begin{bmatrix} \ddot{x}_a \\ \ddot{x}_b \end{bmatrix}=\begin{bmatrix} F_a \\ F_b \end{bmatrix}=\begin{bmatrix} -(c_{aa}\dot{x}_a+c_{ab}\dot{x}_b+k_{aa}x_a+k_{ab}x_b) \\ m_{bbs}\ddot{x}_b \end{bmatrix} \tag{10}$$

Examination of the second of Eq. (10) shows that the correct solution for $\ddot{x}_b$ will not be obtained. The effect of the erroneous $\ddot{x}_b$ on $\ddot{x}_a$ will be felt through the $m_{ab}\ddot{x}_b$ term in Eq. (3) and Eq. (10). To correct this problem, set m_{ba} and m_{bbh} to 0. This will give the correct solution for $\ddot{x}_b$ and will not affect the first of Eq. (10) which becomes

$$\begin{bmatrix} m_{aa} & m_{ab} \\ 0 & m_{bbs} \end{bmatrix}\begin{bmatrix} \ddot{x}_a \\ \ddot{x}_b \end{bmatrix}=\begin{bmatrix} -(c_{aa}\dot{x}_a+c_{ab}\dot{x}_b+k_{aa}x_a+k_{ab}x_b) \\ m_{bbs}\ddot{x}_b \end{bmatrix} \tag{11}$$

This equation is used to solve the accelerations $\ddot{x}_a$ and $\ddot{x}_b$ finally. This method is suggested because it is the easiest way to implement. Without changing the solution procedure, the row of the hydrodynamic mass matrix corresponding to an input node can be zeroed out before m_h and m_s are added and then the matrix sum inverted. This routine is incorporated in the SHOCK program (Gabrielson 1966) to get the dynamic response of lumped mass system.

4. Analysis

4.1. Model development

In the detailed core model, the fuel assemblies are modeled as uniform beams. Lumped masses are included at spacer grid locations to represent the significant modes of vibration of the fuel and to account for possible spacer grid impacting. Nonlinear spring coupling are used to simulate the gaps in the core. Each spacer grid is characterized by the dual load path model which represents the load paths associated with both one-sided and through-grid impacts. One-sided loads are the loads experienced by one side of a grid when it impacts on another grid or the core shroud. Through-grid loads are the loads developed through grid loadings on a spacer grid.

The fuel analytical model was constructed by calculating nodal properties for corresponding locations based on the weight distribution data. The dynamic characteristics of the fuel bundle including natural frequency and damping were also determined from the test data. The analytical model of the fuel bundle was modified to include dynamic effects by adjusting the bundle stiffness to obtain the proper natural frequency and prescribing the damping as a percentage of critical damping.

Hydrodynamic (diagonal coupling coefficients) mass was added to the structural mass to obtain the proper natural frequency in water. The off-diagonal coupling terms are not considered in the core model, that is hydraulic coupling between the fuel assemblies is neglected. This was justified by water loop tests (Stokes and King 1978), which indicate that the natural frequency drop can be accounted for by added masses corresponding to the displaced liquid, meaning that a fuel assembly in a channel does not behave in a significantly different manner as a fuel assembly in an infinite fluid. Physically this means that without a wrapper tube, the fluid can flow from one side of the assembly to the other, across the fuel assembly rather than around it.

The spacer grid model was developed considering impacting of adjacent fuel assemblies or peripheral assemblies and the core shroud. If two fuel assemblies hit each other or if one assembly strikes the core shroud, then the spacer grids are loaded with only one force. This type of impact has been called a one-sided impact. The second impact type is called a through-grid impact because the impact force is applied simultaneously to opposite faces of the spacer grid. For example, a through-grid impact occurs when one fuel assembly is lying against the core shroud and a second assembly hits it (Jhung, et al. 1992a). Therefore, the spacer grid model separates out through-grid and one-sided load paths (Fig. 4). The pluck vibration, pluck impact, spacer grid compression, and spacer grid section drop tests provide data used in determining the spacer grid impacting parameters.

In order to satisfy current regulatory requirements for load combinations (USNRC 1980) five separate models are developed for the 5, 9, 11, 13 and 15 fuel assembly rows across the core. Core model of fifteen row fuel assemblies is shown in Fig. 5.

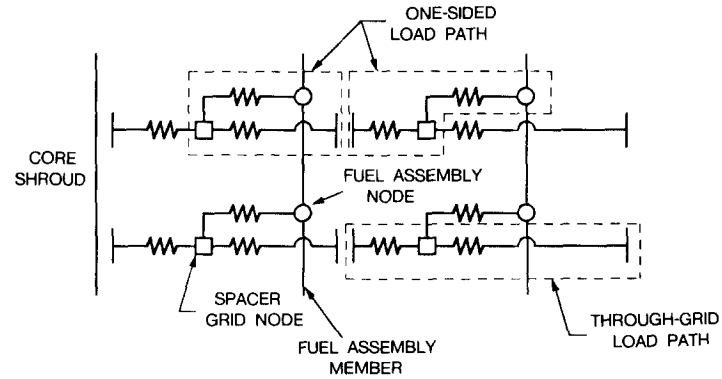

Fig. 4 Dual load path impact model of spacer grid.

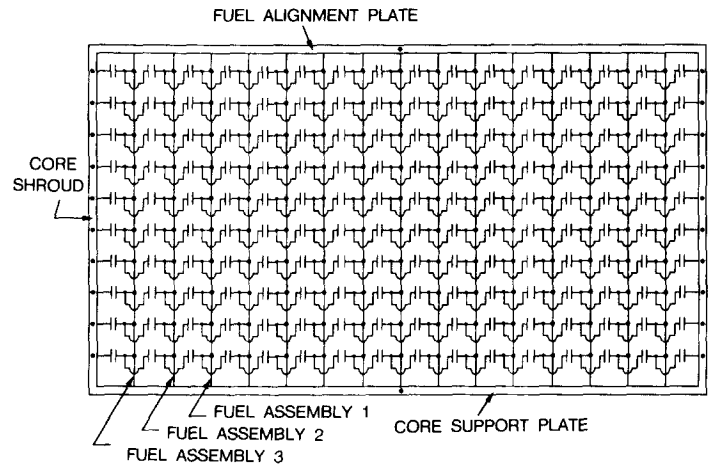

Fig. 5 Core model of 15 row fuel assemblies.

4.2. Input excitations

The input excitations to the detailed core model consist of the translational and angular motions of the core plates and the translational motion of the core shroud. The core shroud is so stiff comparing with fuel assembly that its local effect is negligible. Therefore, only the translational component of the core shroud is used. The input motions are obtained from a seismic analysis of a coupled internals and core model which has a much less detailed representation of the core (Jhung and Hwang 1993).

Fig. 6. shows the acceleration time histories of the reactor vessel flange and snubber, the fuel alignment plate and the core support plate. The reactor vessel motions are used to excite the coupled internals and core model, the result of which analysis is the core plate motions which is amplified by approximately 3 times from the reactor vessel motions. The core support plate motion is almost half of the fuel alignment plate motion but the relative displacement time histories of the core plates to the reactor vessel flange, as shown in Fig. 7, show that the core support plate is excited more severely than the fuel alignment plate. This is explained by the fact that all components of the reactor internals including fuel assemblies behave like a pendulum with several lumped masses for seismic excitations (Jhung, et al. 1992b).

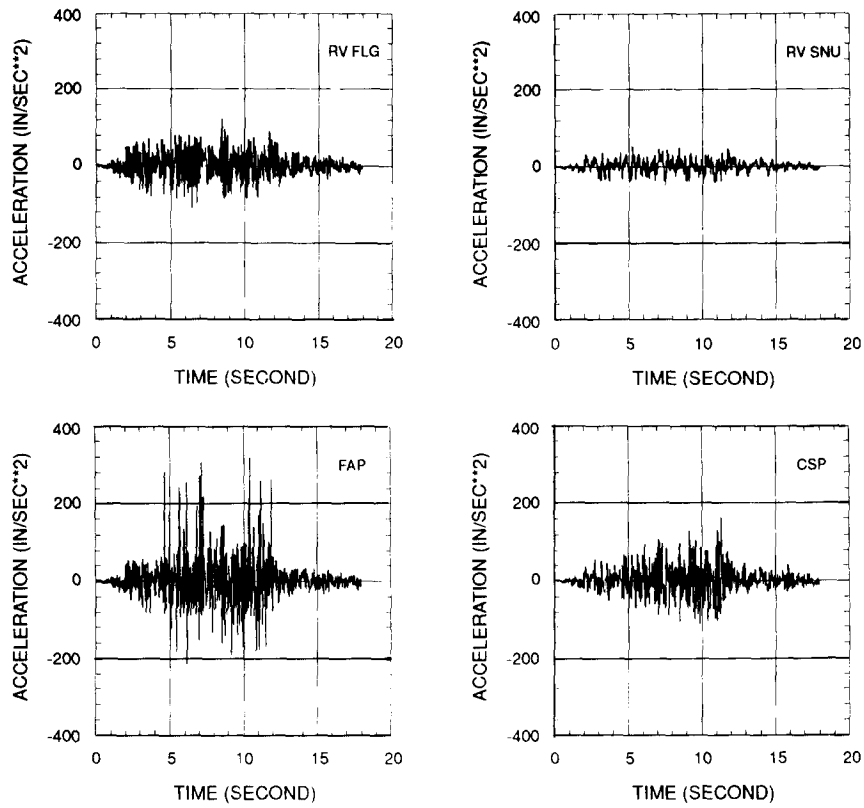

Fig. 6 Acceleration time histories for seismic excitation.

The response spectra at the reactor vessel and the core plates are shown in Fig. 8. The spectra contents are almost same for the frequency ranges between 1 to 6 Hz which fall on the first several significant modes of the fuel assembly. The natural frequencies of the reactor internals are above 8 Hz and so the response contents are not altered below 8 Hz in the frequency domain from the analysis of the coupled internals and core model. This gives a possibility of the analysis of the reactor core using the reactor vessel motions directly not performing a coupled internals and core analysis.

The input motions of the operating basis earthquake for the Ulchin nuclear power plant units 3 and 4 in Korea are used to get the fuel assembly response and the input excitations of the operating basis earthquake are increased by 25% to get the response characteristics.

4.3. Dynamic responses

The responses of the fuel assemblies to the excitations were obtained using the SHOCK code, which integrates the equations of motion by the Runge-Kutta-Gill method for first-order differential equations and provides the time-history response of the fuel assemblies (Kuo 1972).

The integration time step was determined based on the impact pulse which is typically estimated to be 10 milliseconds for the seismic excitation. The number of steps per pulse will be $(10\times10^{-3})/(2\times10^{-4})=50$ for the constant time step of 2×10^{-4} second, which is large enough for this kind of analysis. In this case, the maximum frequency range encompassed is $[2\pi(20)(2\times10^{-4})]^{-1}=39.8$

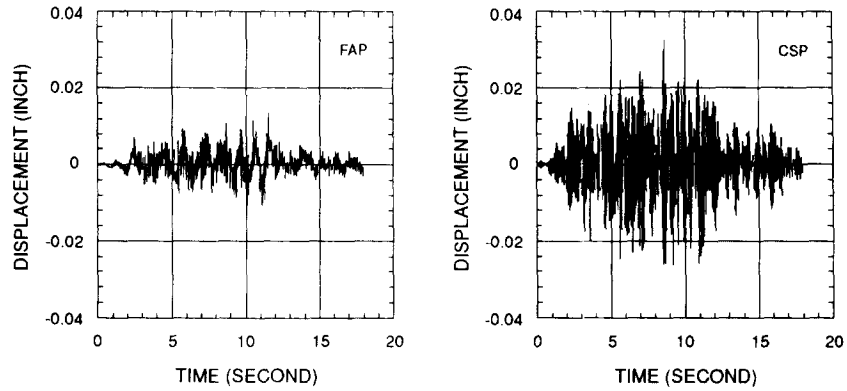

Fig. 7. Relative displacement time histories of core plates to reactor vessel flange.

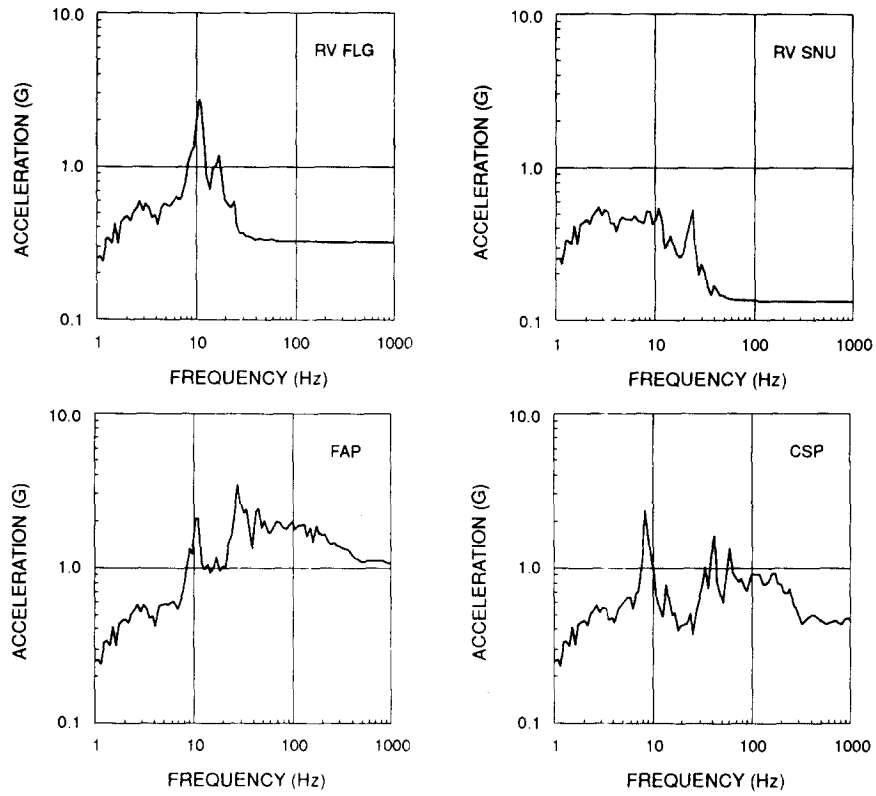

Fig. 8 Response spectra for seismic excitation.

Hz because time step is almost equal to (1/20)×(minimum period τ) (ASCE 1986). The 39.8 Hz is wide enough to cover the fuel assembly frequencies because fuel assembly responds to the seismic excitation by moving back and forth approximately at the first mode frequency of 1 Hz.

5. Results and discussion

The result of the core analysis consists of peak spacer grid impact loads and fuel assembly

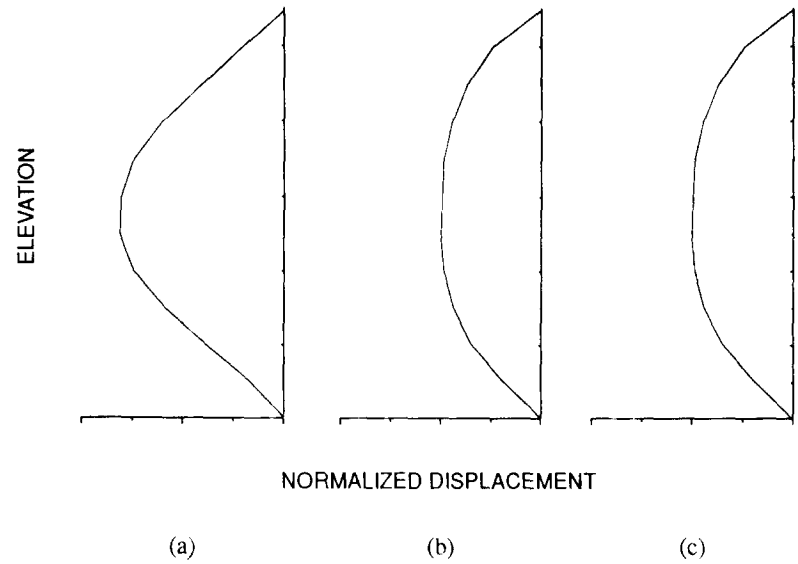

Fig. 9 Deflected shapes of fuel assembly for peak loading conditions: (a) peak displacement; (b) peak moment; (c) peak shear.

deflected shapes. The impact loads are used to evaluate the structural integrity of spacer grids. The fuel assembly deflected shapes which correspond to peak loading conditions-peak displacement, peak shear and peak moment-are used to calculate stresses using a detailed static model of the fuel assembly. The deflected shapes, as shown in Fig. 9, for OBE excitation indicate that the fuel assemblies respond to the seismic excitation by moving back and forth across the core at approximately their first mode natural frequencies. Fig. 10 shows the time histories of the impact loads acting on the center spacer grids for a short time period. It is clearly seen that the magnitude of the spacer grid impact force decreases as a fuel assembly gets away from the core shroud. Or, the peripheral fuel assembly carries the largest dynamic responses. This is due to the large gap separating the peripheral fuel assembly and the core shroud, allowing more horizontal motions than interior fuel assemblies. This is clear in Fig. 12 which shows the fuel assembly number where the maximum responses are obtained.

The spacer grid impact loads at 10 elevations for two adjacent fuel assemblies are shown in Fig. 11. The peak impact is found at the spacer grid located in the middle of the fuel assembly.

Table 1 gives the impact histories for OBE×2.0 excitations; each cell contains the number of occurrence of the impact force between the center spacer grids of the various assemblies in the row. For example, 6 one-sided impacts for the spacer grid (right side) of fuel assembly 15 have a maximum force less than $0.4F_{max}$; 2 impacts have a maximum force between $0.4F_{max}$ and $0.5F_{max}$, etc. For the one-sided forces, the impacts on the left and right side of the grid are independent. The damage such as plastic deformation (if any) to a grid from an one-sided impact occurs to the first few cells, i.e., a left-sided impact does not affect the right side of the grid.

The spacer grid impact loads and the fuel assembly responses are shown in Figs. 13 and 14, respectively, for core models with different number of fuel assembly rows. The maximum responses occur in the longest rows. This is due to enough time for the 15 row fuel assemblies to be piling-up. If there is no pile-up, or no spacer grid impact load, the longest row and

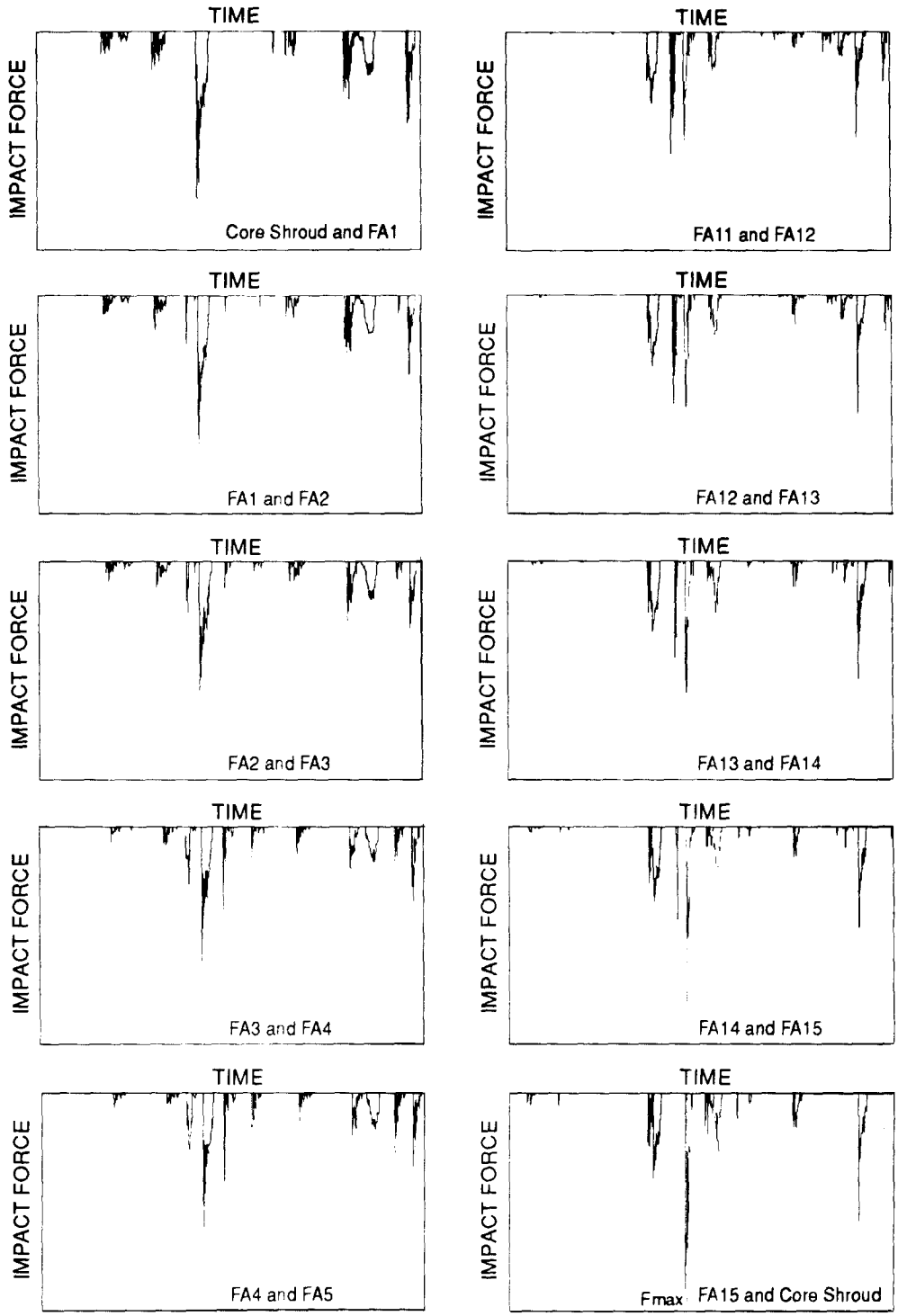

Fig. 10 Impact force on the center spacer grid of fuel assemblies.

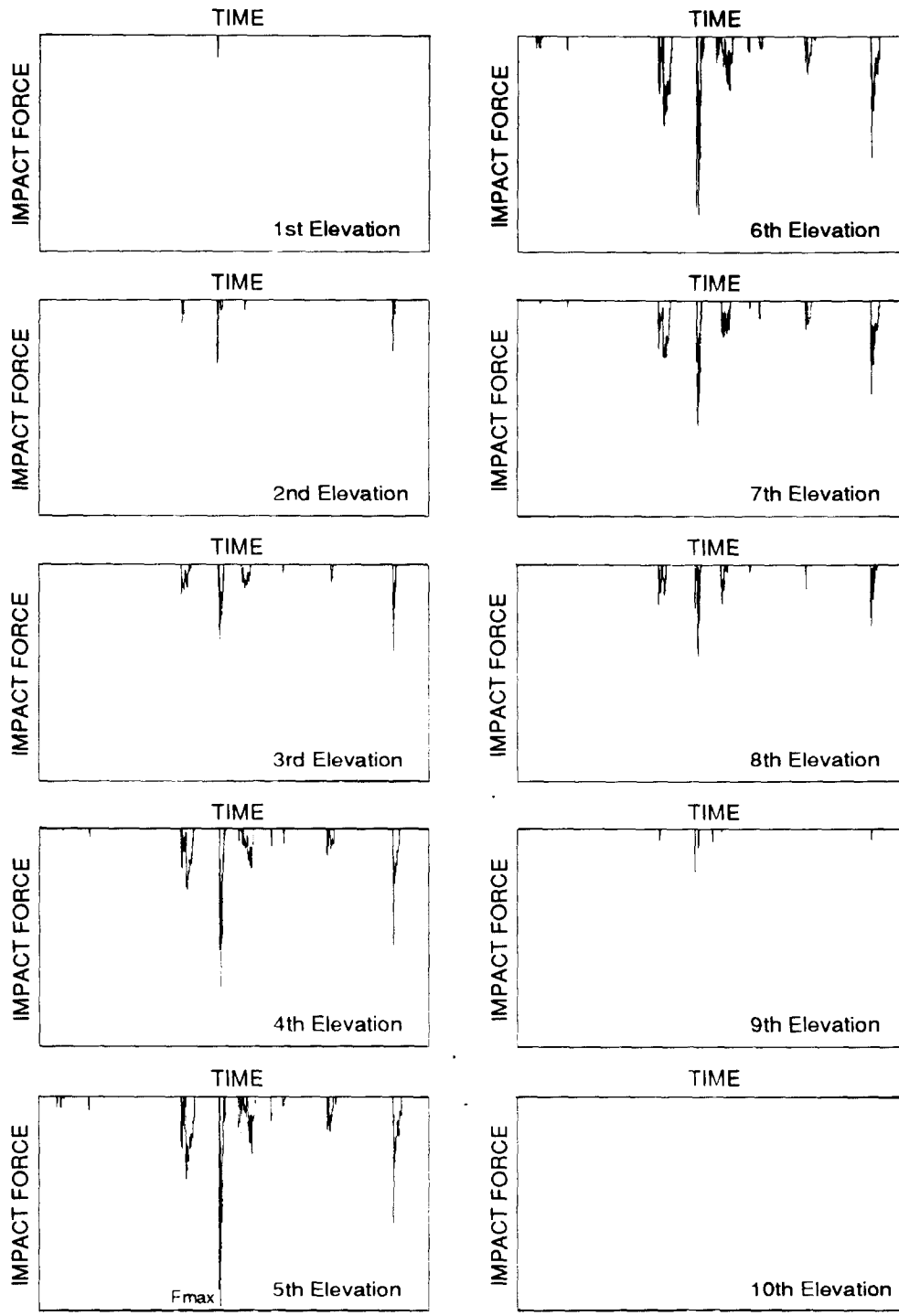

Fig. 11 Impact force on the spacer grid at each elevation.

Table 1 Impact force histories at center spacer grid nodes

	One-sided impact														Through-grid impact						
	Left side							Right side													
$\%F_{max}$	40	50	60	70	80	90	100	40	50	60	70	80	90	100	40	50	60	70	80	90	100
Fuel assy 1	8	3	0	1				5	1	1					2	1					
Fuel assy 2	6	0	1					5							1	1	1				
Fuel assy 3	6	0	1					6							1	1					
Fuel assy 4	9	0	1					4	2						1	1					
Fuel assy 5	2	3	1					6	2						1	1					
Fuel assy 6	4	3	1					5	3	1					2						
Fuel assy 7	6	4	0	1				4	3	2					5						
Fuel assy 8	7	3	2	1				4	3	1	1				4						
Fuel assy 9	3	4	3	1				6	2	3	1				3						
Fuel assy10	7	2	4	1				7	4	2	1				3						
Fuel assy11	7	4	0	1				9	2	2					4	1					
Fuel assy12	7	1	2					5	2	2					3	2					
Fuel assy13	6	1	2					5	4						1	2	1				
Fuel assy14	4	3						4	3	2					1	3	1				
Fuel assy15	4	1	1	1	1			6	2	1	1	1	0	1*	3	1	1				

*$=F_{max}$

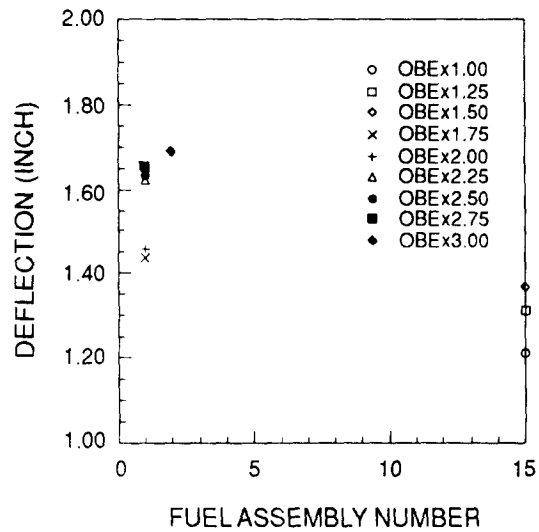

Fig. 12 Maximum fuel assembly deflections along the row.

the shortest row fuel assembly models produce the same response as in the case of the analysis for the secondary side pipe break (Jhung, et al. 1992b).

The maximum spacer grid and fuel assembly responses are shown in Fig. 15 with respect to the intensity of input motions. As the input motion increases linearly, the response increases almost linearly. Therefore the non-linearity of the fuel assembly response due to the seismic excitation is not significant.

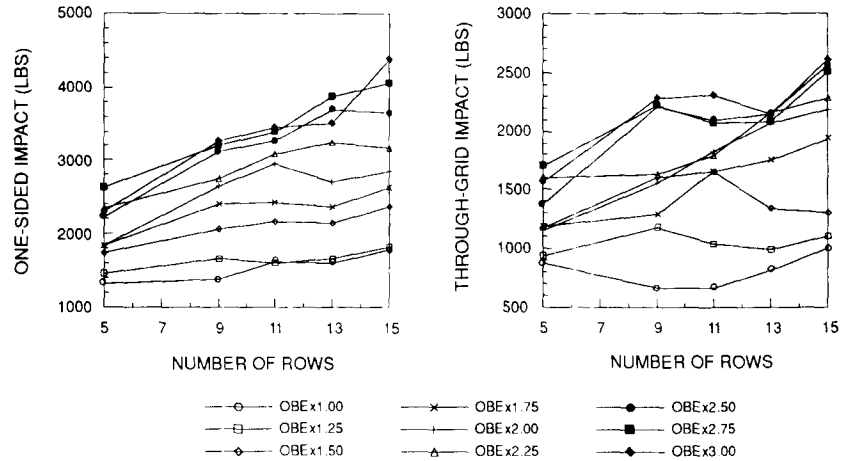

Fig. 13 Variations of spacer grid impact loads per number of rows.

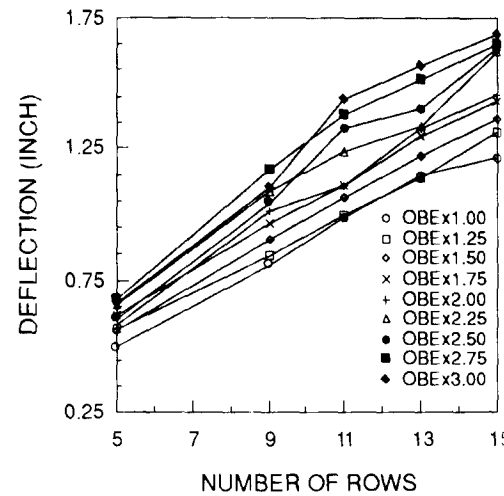

Fig. 14 Variations of fuel assembly deflections per number of rows.

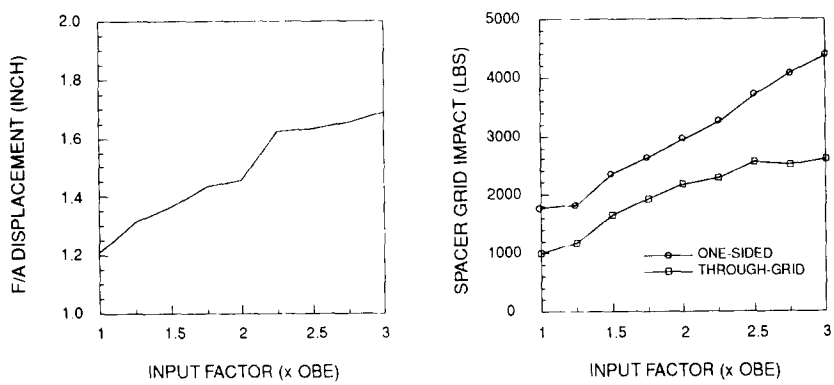

Fig. 15 Variations of maximum responses per input excitations.

6. Conclusions

Dynamic analyses of the reactor core were performed for the seismic excitations for various rows of fuel assembly models and variations of input intensity. The following conclusions were obtained:

1. Fuel assemblies in the longest rows experience the severest response for the seismic excitations, so it is necessary to perform analysis for the longest row model to get design loads.
2. The maximum fuel assembly responses occur at the core periphery. For the beam-column analysis of a fuel assembly the peripheral fuel assembly should be chosen for the worst case.
3. The maximum fuel assembly deformations occur in the middle of the fuel assembly height. To guarantee the control rod insertion during earthquake this maximum deformation should not exceed the criteria.
4. The maximum impact loads are found on the spacer grid located at the center of the fuel assembly. Therefore it is necessary to increase the strength of the center spacer grids for severer seismic excitation.

References

ASCE (1986), *Standard for Seismic Analysis of Safety-Related Nuclear Structures*, American Society of Civil Engineers, New York.

Chen, S. S. (1975), "Vibrations of nuclear fuel bundles", *Nuclear Engineering and Design*, **35**, 399-422.

Gabrielson, V. K. (1966), "SHOCK-A computer code for solving lumped-mass dynamic systems", Technical Report SCL-DR-65-34, Sandia Laboratories, Livermore, CA.

Jhung, M. J., Song, H. G. and Park, K. B. (1992a), "Dynamic characteristics of spacer grid impact loads for SSE", *Journal of the Korean Nuclear Society*, **24**(2), 111-120.

Jhung, M. J., Park, K. B. and Sohn, G. H. (1992b), "Dynamic analysis of the reactor core for pipe break and seismic excitations", *Proceedings of the 7th International Conference on Pressure Vessel Technology*, Düsseldorf, Germany, June.

Jhung, M. J. and Hwang, W. G. (1993), "Seismic design criteria for the reactor vessel internals of the Korean Standard Nuclear Power Plant", *Proceedings of the Seminar on Pressure Vessel and Piping Technology*, Singapore, May.

Kuo, S. S. (1972), *Computer Applications of Numerical Methods*, Addison-Wesley, New York.

Queval, J. C., Gantenbein, F. and Rigaudeau, J. (1991), "Experimental studies on seismic behavior of PWR fuel assembly rows", *Seismic Engineering-1991*, ASME PVP **220**, 255-260.

Stokes, F. E. and King, R. A. (1978), "PWR fuel assembly dynamic characteristics", BNES, Vibration in Nuclear Plants, Keswick, UK.

USNRC, (1980), "Methodology for combining dynamic responses", NUREG-0484, Rev. 1, US Nuclear Regulatory Commission, New York.